EJSIT
European Journal of Science, Innovation and Technology
ISSN: 2786-4936
www.ejsit-journal.com
Volume 6 | Number 4 | 2026

Effects of Heat Treatment on the Physical Properties and Stress Wave-Based Dynamic Modulus of Elasticity of Camphor Wood (*Cinnamomum camphora*): A Response Surface Methodology Approach

Duc Tu Nguyen[1], Thi Kim Hong Tang[1*], Van Doan Duong[2], and Nhat Quang Nguyen[1]
[1]Nong Lam University – Ho Chi Minh City, Vietnam
[2]Thai Nguyen University, Vietnam

ABSTRACT

This study investigated the effects of dry-air and hydrothermal heat treatments on the physical properties and stress wave-based dynamic modulus of elasticity (DMOE) of Camphor wood (*Cinnamomum camphora*) using response surface methodology (RSM). Dry-air treatment was conducted at 150 – 200 °C for 10 – 20 h, whereas hydrothermal treatment was performed at 120 – 150 °C for 60 – 120 min. Equilibrium moisture content (EMC), air-dry density (AD), and stress wave-based DMOE were determined after treatment. Treatment temperature and duration significantly affected the measured properties, although their relative importance varied between the two treatment methods. Increasing treatment severity generally resulted in reductions in EMC, AD, and DMOE. Response surface models adequately described the relationships between the processing variables and the measured responses. Multi-response optimization was subsequently used to identify suitable treatment conditions by considering EMC, AD, and DMOE simultaneously. The optimized conditions differed between the dry-air and hydrothermal processes, reflecting differences in their responses to treatment temperature and duration. The results demonstrate the potential of stress wave-based DMOE as a rapid, non-destructive indicator for characterizing changes in the dynamic stiffness of heat-treated Camphor wood and provide a basis for selecting suitable thermal modification conditions for this species.

Keywords: Camphor wood; dynamic modulus of elasticity; response surface methodology; stress wave; thermal modification

INTRODUCTION

Heat treatment has become one of the most promising environmentally friendly wood modification technologies because it enhances wood performance without the use of chemical preservatives. Thermal modification alters the chemical composition of the wood cell wall, particularly through the degradation of hemicelluloses, resulting in reduced hygroscopicity, lower equilibrium moisture content (EMC), improved dimensional stability, and enhanced biological durability, thereby extending the service life of wood products (Acosta et al., 2021; Jančíková & Jablonský, 2025). Compared with conventional chemical modification processes, thermal modification is regarded as a sustainable technology that meets the growing demand for environmentally friendly wood products (Acosta et al., 2021; Jančíková & Jablonský, 2025). Depending on the heat-transfer medium, thermal modification can be performed under dry-air or hydrothermal conditions, each inducing distinct physicochemical changes and consequently different effects on wood properties (Esteves & Pereira, 2009; Hill, 2006; Jančíková & Jablonský, 2025).

Numerous studies have shown that thermal modification significantly influences the physical and mechanical properties of many commercial wood species, including western

*Corresponding Author: tangkimhong@hcmuaf.edu.vn (T.K.H. Tang)

hemlock, *Cryptomeria japonica*, oak, ayous, iroko, and beech. In general, increasing treatment severity reduces EMC and wood density owing to the degradation of cell-wall constituents, although excessive treatment severity may adversely affect mechanical performance (Esteves et al., 2025; Laskowska et al., 2025; Nakagawa et al., 2024; Tomak & Ermeydan, 2025; Vidholdová et al., 2026). Hydrothermal treatment has recently attracted increasing attention because the presence of water or steam modifies heat-transfer characteristics and may alleviate excessive thermal degradation under certain treatment conditions (Laskowska et al., 2025; Vidholdová et al., 2026). These findings indicate that treatment temperature, duration, and heating medium interact to determine the final properties of thermally modified wood. Consequently, statistical optimization approaches such as response surface methodology (RSM) provide an efficient means of simultaneously evaluating multiple processing variables while reducing the number of experimental trials.

Camphor wood (*Cinnamomum camphora*) is derived from an evergreen hardwood species occurring naturally in Japan, the Ryukyu Islands, southern China, Hainan, Taiwan, and Vietnam. The species is cultivated in many tropical and subtropical countries and has also become naturalized in Australia (Windadri & Rahayu, 1999). Owing to its characteristic fragrance, attractive wood, and value for cabinet work, *C. camphora* has potential for various value-added wood applications (Windadri & Rahayu, 1999; Cipta et al., 2022; Wang et al., 2023). Previous studies have shown that thermal modification can reduce the equilibrium moisture content of Camphor wood through heat-induced changes in the wood cell wall while maintaining acceptable mechanical performance under moderate treatment conditions (Sun et al., 2022). However, published studies on *C. camphora* have focused primarily on its essential oils, medicinal applications, and chemical constituents, whereas research addressing the thermal modification and engineering performance of its stem wood remains comparatively limited.

In addition to improving wood properties, reliable and rapid techniques are required to evaluate the effects of thermal modification without damaging the material. Among the available non-destructive evaluation (NDE) methods, stress wave testing has been widely employed for determining the dynamic modulus of elasticity (DMOE) because it is rapid, simple, and suitable for repeated measurements on the same specimen before and after treatment. Previous studies have shown that stress wave measurements are sensitive to changes induced by thermal modification and can effectively detect variations in the stiffness and density of heat-treated wood. For example, Garcia et al. (2012) reported significant changes in stress wave-based DMOE, air-dry density, and EMC of thermally modified *Eucalyptus grandis*, whereas Del Menezzi et al. (2014) demonstrated the applicability of stress wave and ultrasonic techniques for evaluating the mechanical behaviour of thermally modified tropical wood.

Although the effects of thermal modification have been investigated for a wide range of wood species, available information for *C. camphora* remains comparatively limited. Existing studies have mainly addressed chemical composition, moisture-related behaviour, and selected physical properties, whereas relatively little attention has been paid to the response of stress wave-based DMOE. Moreover, most published studies have evaluated individual treatment conditions rather than systematically investigating the interactive effects of heat-treatment method, temperature, and duration. Consequently, the combined influence of these processing variables on the physical properties and stress wave-based DMOE of Camphor wood remains insufficiently understood, highlighting the need for a systematic optimization approach.

Therefore, the present study investigated the effects of dry-air and hydrothermal heat treatments on the physical properties and stress wave-based dynamic modulus of elasticity of Camphor wood using response surface methodology. Specifically, the effects of treatment

temperature and duration on EMC, air-dry density, and DMOE were evaluated, and response surface models were developed to quantify the interactions among processing variables and identify optimum treatment conditions. The results provide a scientific basis for optimizing the thermal modification of Camphor wood and expand the application of stress wave-based non-destructive evaluation for assessing thermally modified hardwoods.

MATERIALS AND METHODS

Camphor Wood Samples

Camphor wood (*Cinnamomum camphora*) timbers were obtained from a wood product manufacturing factory in Ho Chi Minh City, Vietnam. Samples were prepared with nominal dimensions of 30 × 100 × 500 mm (thickness × width × length). For the dry-air heat treatment, the samples were kiln-dried at 60 °C for 5 days to achieve a moisture content of approximately 12 – 15% before treatment. In contrast, the samples assigned to the hydrothermal treatment were subjected directly to the treatment process without prior kiln drying.

The samples were randomly assigned to the experimental groups according to the response surface methodology (RSM) design. Each treatment condition consisted of five replicate samples, together with an untreated control group.

Experimental Design

Response surface methodology (RSM) employing a central composite design (CCD) was used to optimize the heat-treatment conditions for dry-air and hydrothermal modification of Camphor wood. For each treatment method, treatment temperature and duration were considered as the independent variables, whereas equilibrium moisture content (EMC), air-dry density (AD), and stress wave-based dynamic modulus of elasticity (DMOE) were used as the response variables. An 11-run CCD was generated separately for each treatment method using Minitab version 21.2 (Minitab LLC, State College, PA, USA), resulting in 11 experimental runs for dry-air treatment and another 11 runs for hydrothermal treatment. Each CCD comprised factorial, axial, and centre points. The investigated ranges were 150 – 200 °C and 10 – 20 h for dry-air treatment, and 120 – 150 °C and 60 – 120 min for hydrothermal treatment. The coded and actual experimental levels of the independent variables are presented in Table 1.

Table 1. Coded and actual levels of the independent variables used in the response surface methodology design

Heat treatment method	Independent variable	Coded level				
		–α	**–1**	**0**	**+1**	**+α**
Dry-air heat treatment	Temperature (°C)	140	150	175	200	210
	Duration (h)	8	10	15	20	22
Hydrothermal heat treatment	Temperature (°C)	114	120	135	150	156
	Duration (min)	48	60	90	120	132

Heat Treatment

Dry-air heat treatment was carried out in a Memmert UN260 laboratory oven (Memmert GmbH, Schwabach, Germany) with a chamber size of 640 × 800 × 500 mm (width × height × depth), whereas hydrothermal heat treatment was performed using a Regmed Digester AUE/E-20 (Regmed Indústria e Comércio Ltda., Osasco, SP, Brazil) equipped with a 360° rotating chamber (220 mm in diameter × 510 mm in depth). Both systems provided automatic temperature control.

The experiments were conducted according to the coded and actual levels of the independent variables presented in Table 1. Throughout the experiments, all operating parameters other than treatment temperature and duration were maintained constant.

Determination of Equilibrium Moisture Content (EMC)

Specimens measuring 20 × 20 × 23 mm (radial × tangential × longitudinal) were prepared from each heat-treatment group, including the untreated control, with five specimens per group. Prior to testing, the specimens were conditioned in a Memmert HPP260eco climate chamber (Memmert GmbH, Schwabach, Germany) maintained at 20 °C and 65% relative humidity until constant mass was attained. The equilibrium mass was recorded as m_{eq}. The specimens were subsequently oven-dried at 103 °C to constant mass using a Memmert UN260 drying oven, and the oven-dry mass was recorded as m_0. Equilibrium moisture content (EMC) was determined in accordance with ASTM D4442-20 (ASTM International, 2025) using Eq. (1).

$$EMC\ (\%) = \frac{m_{eq} - m_0}{m_0} \times 100\% \quad (1)$$

where m_{eq} is the equilibrium mass (g), and m_0 is the oven-dry mass (g).

Determination of Air-Dry Density and Stress Wave-Based Dynamic Modulus of Elasticity

Air-dry density (AD) and stress wave-based dynamic modulus of elasticity (DMOE) were determined using specimens measuring 20 × 20 × 320 mm (radial × tangential × longitudinal). Five specimens were prepared for each heat-treatment group, including the untreated control. Before testing, the specimens were conditioned at 20 °C and 65% relative humidity until constant mass was attained.

The air-dry density was determined by dividing the conditioned mass of each specimen by its corresponding volume under the same conditioning environment.

Stress wave measurements were carried out using a Fakopp Microsecond Timer (Fakopp Enterprise, Agfalva, Hungary). Longitudinal stress waves were generated by striking the transmitting transducer with a hammer, and the wave propagation time was recorded by the receiving transducer. Each specimen was measured five times, and the mean propagation time was used to calculate the stress wave velocity (SWV) according to Eq. (2):

Stress wave velocity was calculated as

$$SWV\ \left(\frac{m}{s}\right) = \frac{L}{t} \quad (2)$$

where L is the specimen length (m), and t is the stress wave propagation time (s).

The stress wave-based dynamic modulus of elasticity was calculated using Eq. (3):

$$DMOE\ (GPa) = AD \times SWV^2 \times 10^{-6} \quad (3)$$

where $DMOE$ is the dynamic modulus of elasticity (GPa); AD is the air-dry density (g/cm^3); SWV is the stress wave velocity (m/s).

Statistical Analysis

Response surface methodology (RSM) analyses were performed separately for the dry-air and hydrothermal heat-treatment processes using Minitab version 21.2. Quadratic polynomial models were developed to describe the relationships between treatment temperature, treatment duration, and the response variables, including equilibrium moisture content (EMC), air-dry density (AD), and stress wave-based dynamic modulus of elasticity (DMOE). Model significance and the effects of individual model terms were evaluated by analysis of variance (ANOVA) at a significance level of $p < 0.05$. Model adequacy was assessed using the coefficient of determination (R^2), adjusted R^2, and lack-of-fit tests. Response surface and contour plots were generated to illustrate the effects of the processing variables on each response. Multi-response optimization based on the desirability function was subsequently performed to determine the optimum processing conditions for both dry-air and hydrothermal heat treatments.

RESULTS AND DISCUSSION

The experimental response values of equilibrium moisture content (EMC), air-dry density (AD), and stress wave-based dynamic modulus of elasticity (DMOE) obtained from the dry-air and hydrothermal heat-treatment experiments, together with those of the untreated control, are presented in Table 2. Within each heat-treatment method, noticeable variations in all response variables were observed among the experimental runs, indicating the influence of treatment temperature and duration. For descriptive purposes, the combined dataset covered ranges of 4.54 – 11.37% for EMC, 0.378 – 0.527 g/cm³ for AD, and 6.60 – 9.50 GPa for DMOE. Because the dry-air and hydrothermal processes were evaluated using independent response surface designs with different operating ranges, the effects of the processing variables were analysed separately for each treatment method in the following sections.

Table 2. Experimental response values of equilibrium moisture content (EMC), air-dry density (AD), and stress wave-based dynamic modulus of elasticity (DMOE) of Camphor wood under dry-air and hydrothermal heat-treatment conditions

Experimental condition		EMC (%)	AD (g/cm³)	DMOE (GPa)
Dry-air heat treatment	140 °C, 15 h	9.32 (0.02)	0.527 (0.007)	9.3599 (0.0195)
	150 °C, 10 h	9.36 (0.17)	0.523 (0.006)	9.0722 (0.0421)
	150 °C, 20 h	8.58 (0.22)	0.433 (0.002)	7.6587 (0.0374)
	175 °C, 8 h	6.55 (0.19)	0.483 (0.052)	8.8887 (0.9799)
	175 °C, 15 h	6.33 (1.18)	0.444 (0.005)	8.5101 (0.6854)
	175 °C, 15 h	6.29 (1.39)	0.465 (0.007)	8.635 (1.1279)
	175 °C, 15 h	6.12 (1.21)	0.459 (0.01)	8.5318 (0.9453)
	175 °C, 22 h	6.12 (1.29)	0.416 (0.07)	6.8494 (2.0995)
	200 °C, 10 h	4.92 (0.12)	0.435 (0.01)	7.6809 (0.746)
	200 °C, 20 h	4.59 (0.2)	0.424 (0.019)	7.3138 (0.845)
	210 °C, 15 h	4.54 (0.08)	0.422 (0.016)	7.2136 (0.5223)
Hydrothermal heat treatment	114 °C, 90 min	11.37 (0.22)	0.516 (0.014)	9.2262 (0.9294)
	120 °C, 60 min	10.83 (0.34)	0.52 (0.001)	9.4767 (0.0629)
	120 °C, 120 min	9.22 (0.09)	0.426 (0.022)	7.3997 (0.5635)
	135 °C, 48 min	9.84 (0.02)	0.527 (0.035)	9.4958 (1.4338)
	135 °C, 90 min	9.44 (0.13)	0.493 (0.01)	8.1377 (0.0154)
	135 °C, 90 min	9.36 (0.16)	0.485 (0.008)	7.8825 (0.0127)
	135 °C, 90 min	9.27 (0.18)	0.482 (0.008)	7.7167 (0.0236)
	135 °C, 132 min	8.25 (0.1)	0.387 (0.013)	7.1855 (0.1399)
	150 °C, 60 min	9.82 (0.17)	0.505 (0.016)	8.545 (0.1418)
	150 °C, 120 min	7.23 (0.22)	0.378 (0.005)	6.5964 (0.5898)
	156 °C, 90 min	8.64 (0.09)	0.395 (0.022)	7.2361 (0.0657)
Untreated control		11.79 (0.19)	0.528 (0.004)	9.539 (0.2422)

Note: Values represent mean (SD) of five replicates.

Effect of Heat-Treatment Conditions on EMC

The effects of treatment temperature and duration on EMC of Camphor wood were evaluated using RSM. The relative importance of the processing variables is illustrated by the Pareto charts of the standardized effects (Fig. 1), where the vertical reference line represents the significance threshold at the 95% confidence level.

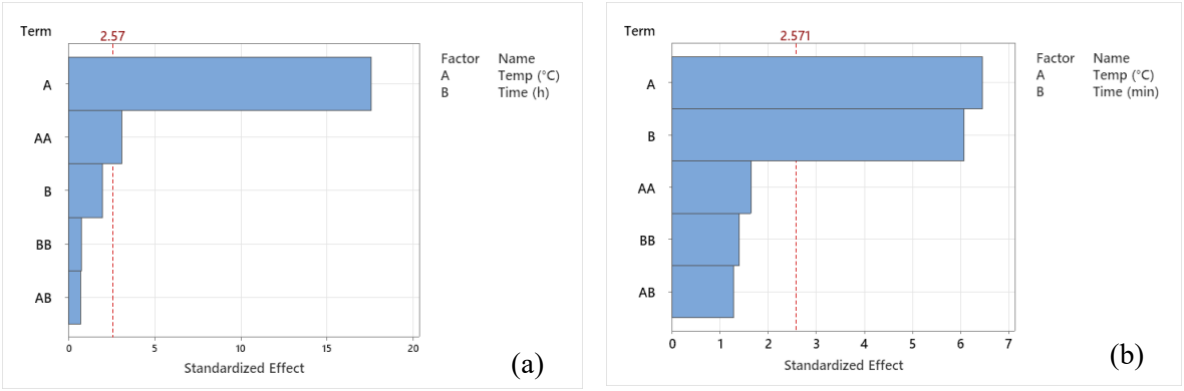

Fig. 1. Pareto charts of the standardized effects of treatment temperature and duration on EMC of Camphor wood during (a) dry-air heat treatment and (b) hydrothermal heat treatment

For the dry-air heat treatment, treatment temperature was identified as the dominant factor affecting EMC (Fig. 1a). The linear effect of temperature was highly significant ($p < 0.001$), whereas treatment duration, the interaction between temperature and duration, and the quadratic effect of treatment duration were not statistically significant ($p > 0.05$). The quadratic effect of temperature remained significant ($p = 0.027$), indicating a slight curvature in the response surface. The fitted quadratic model showed excellent agreement with the experimental data, with an R^2 of 98.48%, an adjusted R^2 of 96.96%, and a predicted R^2 of 89.54%. In addition, the lack-of-fit was not significant ($p = 0.074$), confirming that the model adequately described the relationship between the processing variables and EMC. Accordingly, the predictive equation for the dry-air process was simplified by retaining only the statistically significant terms:

$$EMC\ (\%) = 0.3813 - 0.002870Temp + 0.000006Temp^2 \quad (4)$$

where $Temp$ is the treatment temperature (°C).

For the hydrothermal heat treatment, both treatment temperature and treatment duration significantly influenced EMC, with temperature exhibiting the greatest standardized effect (Fig. 1b). The quadratic and interaction terms were not statistically significant ($p > 0.05$). The fitted model explained 94.55% of the experimental variability, with an adjusted R^2 of 89.10% and a predicted R^2 of 61.76%. Although the regression model was statistically significant ($p = 0.004$), the significant lack-of-fit ($p = 0.029$) indicates that the predictive performance of the model was comparatively weaker than that of the dry-air model. Therefore, only the statistically significant linear terms were retained in the simplified predictive equation:

$$EMC\ (\%) = 0.1959 - 0.000575Temp - 0.000271Time \quad (5)$$

where $Temp$ is the treatment temperature (°C), and $Time$ is the treatment duration (min).

The response surface and contour plots (Fig. 2a,b) show that EMC decreased progressively with increasing temperature during dry-air heat treatment, whereas the influence of treatment duration was relatively limited within the investigated range. The nearly vertical contour lines further confirm that temperature exerted a much stronger influence on EMC than duration. In contrast, the response surface and contour plots for the hydrothermal process (Fig. 2c,d) indicate that both temperature and duration significantly influenced EMC, although temperature remained the dominant factor. These observations are in good agreement with the Pareto charts and the fitted regression models.

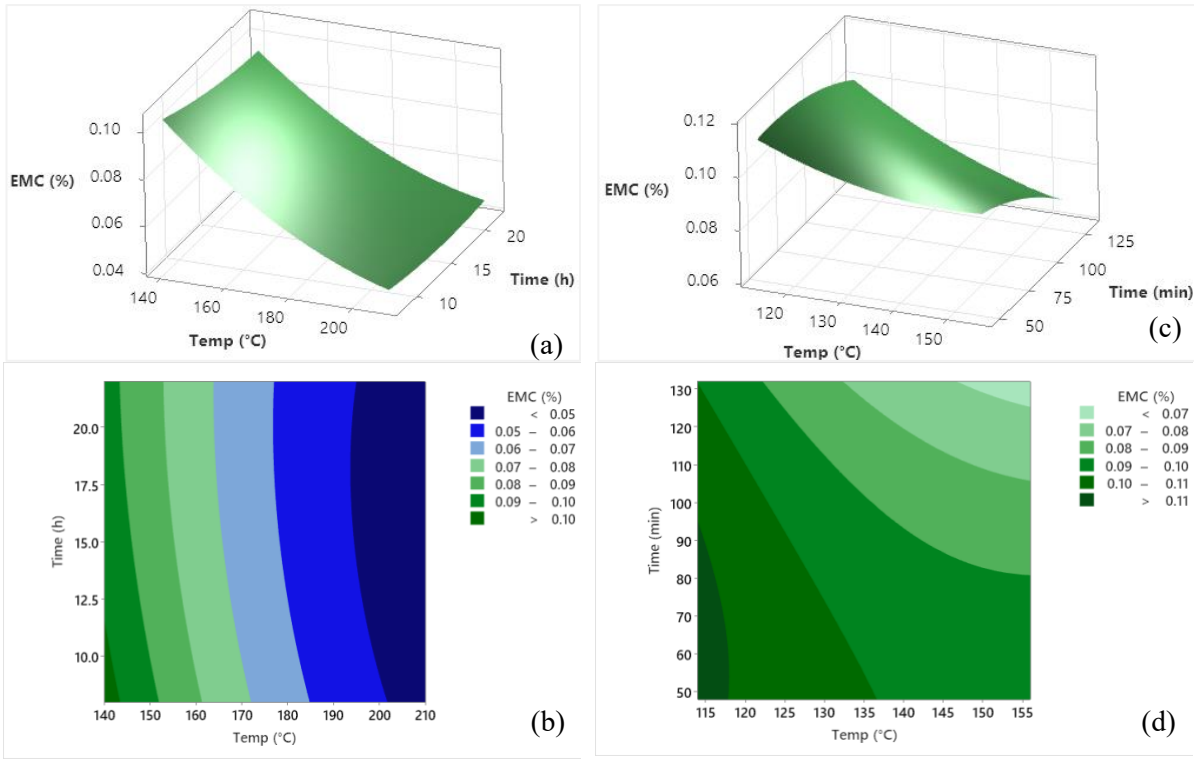

Fig. 2. Response surface and contour plots of EMC as affected by treatment temperature and duration during (a, b) dry-air heat treatment and (c, d) hydrothermal heat treatment of Camphor wood. Panels (a) and (c) present the response surface plots, whereas panels (b) and (d) present the corresponding contour plots.

The reduction in EMC following heat treatment can be attributed primarily to irreversible physicochemical changes within the wood cell wall. Elevated temperatures promote the degradation of hemicelluloses through deacetylation and depolymerization, while reducing the availability and accessibility of moisture-binding sites within the cell wall (Boonstra & Tjeerdsma, 2006; Jančíková & Jablonský, 2025; Tjeerdsma & Militz, 2005). Heat treatment may also increase the relative crystallinity of cellulose and induce structural changes in lignin, including polycondensation and crosslinking reactions, which can further affect the accessibility of water to the cell-wall polymers and reduce wood hygroscopicity (Bhuiyan & Hirai, 2005; Esteves & Pereira, 2009; Hill et al., 2021; Jančíková & Jablonský, 2025). Under hydrothermal conditions, the formation of acetic and formic acids during hemicellulose degradation promotes further degradation of hemicelluloses and contributes to mass loss (Ali et al., 2021). Collectively, these chemical and structural changes reduce the affinity of the wood cell wall for water, resulting in the lower EMC observed after both dry-air and hydrothermal heat treatments.

Effect of Heat-Treatment Conditions on AD

The effects of treatment temperature and duration on AD of Camphor wood were evaluated using RSM. The relative importance of the processing variables is illustrated by the Pareto charts of the standardized effects (Fig. 3), where the vertical reference line represents the significance threshold at the 95% confidence level.

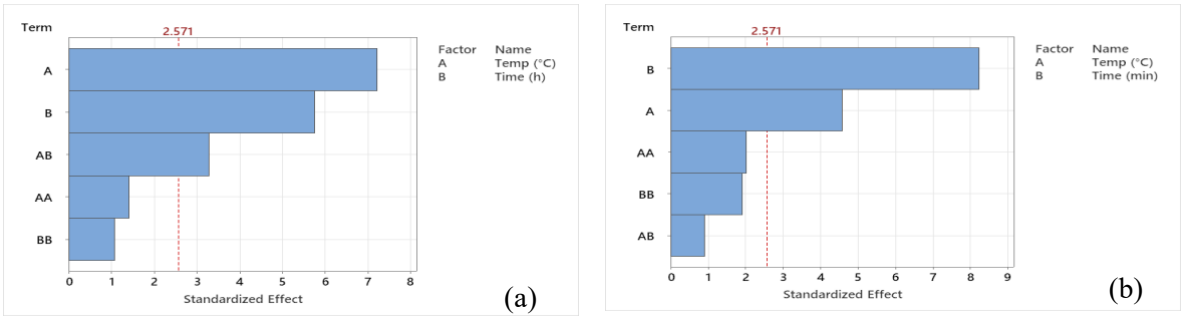

Fig. 3. Pareto charts of the standardized effects of treatment temperature and duration on AD of Camphor wood during (a) dry-air heat treatment and (b) hydrothermal heat treatment

For the dry-air heat treatment, both treatment temperature and treatment duration significantly affected AD, with temperature exhibiting the largest standardized effect, followed by treatment duration and their interaction (Fig. 3a). The linear effects of temperature (p = 0.001) and duration (p = 0.002), together with their interaction (p = 0.022), were statistically significant, whereas the quadratic terms were not significant (p > 0.05). The fitted quadratic model adequately described the experimental data, yielding an R^2 of 95.25%, an adjusted R^2 of 90.51%, and a predicted R^2 of 73.72%. Furthermore, the lack-of-fit was not significant (p = 0.444), indicating satisfactory agreement between the model predictions and the experimental observations. Accordingly, only the statistically significant terms were retained in the simplified predictive equation:

$$AD\ (g/cm^3) = 1.162 - 0.003602Temp - 0.03257Time + 0.000158Temp \times Time \quad (6)$$

where $Temp$ is the treatment temperature (°C), and $Time$ is the treatment duration (h).

For the hydrothermal heat treatment, treatment duration became the dominant factor influencing AD, followed by treatment temperature (Fig. 3b). Both linear terms were statistically significant (p < 0.01), whereas the quadratic and interaction terms were not significant (p > 0.05). The fitted model explained 95.04% of the experimental variability, with an adjusted R^2 of 90.08% and a predicted R^2 of 65.68%. The lack-of-fit was not statistically significant (p = 0.059), confirming that the model adequately represented the experimental responses within the investigated design space. The simplified predictive equation is expressed as:

$$AD\ (g/cm^3) = 0.8870 - 0.001956Temp - 0.001755Time \quad (7)$$

where $Temp$ is the treatment temperature (°C), and $Time$ is the treatment duration (min).

The response surface and contour plots (Fig. 4a,b) show that AD decreased progressively with increasing temperature during dry-air heat treatment, while longer treatment durations further enhanced the reduction in density, particularly at higher temperatures. The curved contour lines indicate a significant interaction between temperature and duration, demonstrating that the influence of one factor depended on the level of the other. In contrast, the response surface and contour plots for the hydrothermal process (Fig. 4c,d) reveal that AD decreased with increasing temperature and treatment duration, with treatment duration exerting a slightly greater influence than temperature, consistent with the Pareto chart. The nearly parallel contour lines further indicate that the interaction between the two variables was negligible, in agreement with the regression analysis.

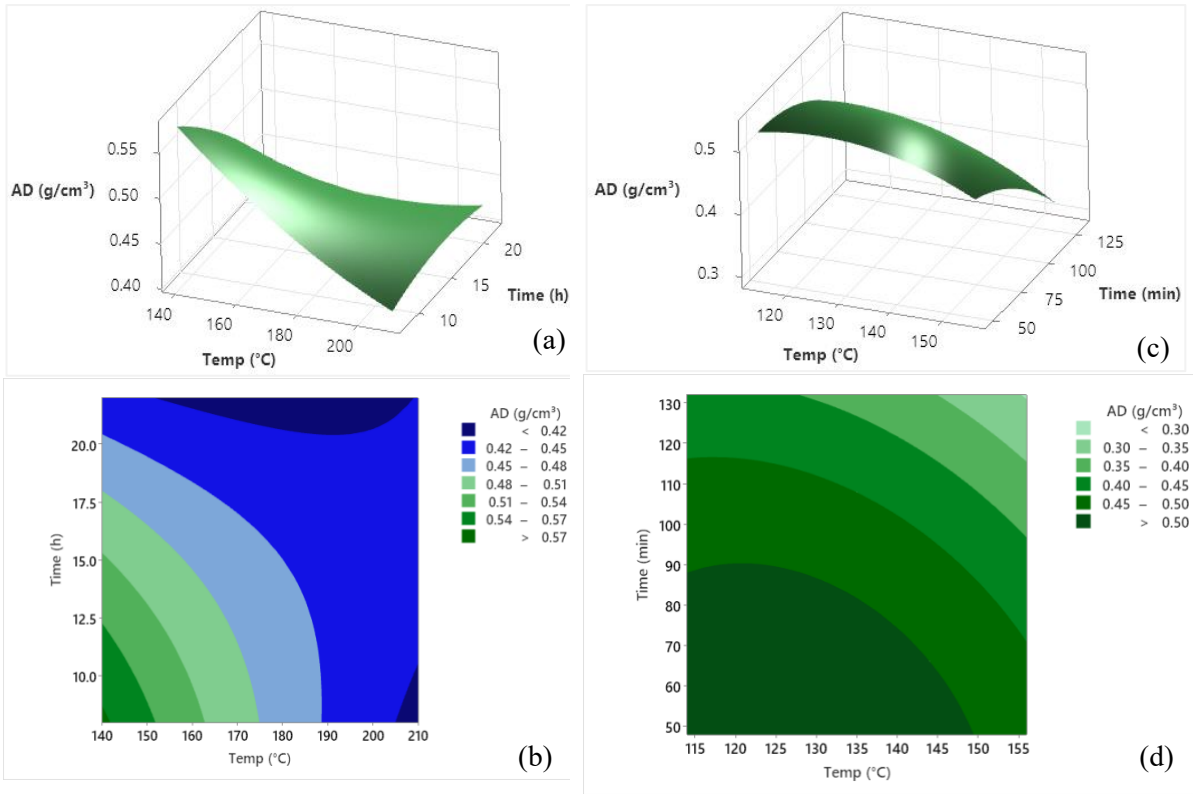

Fig. 4. Response surface and contour plots of AD as affected by treatment temperature and duration during (a, b) dry-air heat treatment and (c, d) hydrothermal heat treatment of Camphor wood. Panels (a) and (c) present the response surface plots, whereas panels (b) and (d) present the corresponding contour plots.

The reduction in air-dry density (AD) after heat treatment is primarily attributed to the thermal degradation of cell-wall components, particularly hemicelluloses, together with the degradation or volatilization of extractives and the release of volatile degradation products. These processes cause mass loss and consequently reduce wood density (Acosta et al., 2021; Esteves & Pereira, 2009; Jančíková & Jablonský, 2025). Under hydrothermal conditions, the formation of acetic and formic acids during hemicellulose degradation promotes further degradation of hemicelluloses and contributes to mass loss, with the extent of mass loss depending on wood species, heating medium, temperature, and treatment duration (Ali et al., 2021). Similar reductions in wood density following thermal modification have been reported for different wood species, and greater treatment severity generally results in greater changes in density (Esteves et al., 2025; Jančíková & Jablonský, 2025).

Effect of Heat-Treatment Conditions on DMOE

The effects of treatment temperature and duration on the stress wave-based dynamic modulus of elasticity (DMOE) of Camphor wood were evaluated using response surface methodology (RSM). The relative importance of the processing variables is illustrated by the Pareto charts of the standardized effects (Fig. 5), where the vertical reference line indicates the significance threshold at the 95% confidence level.

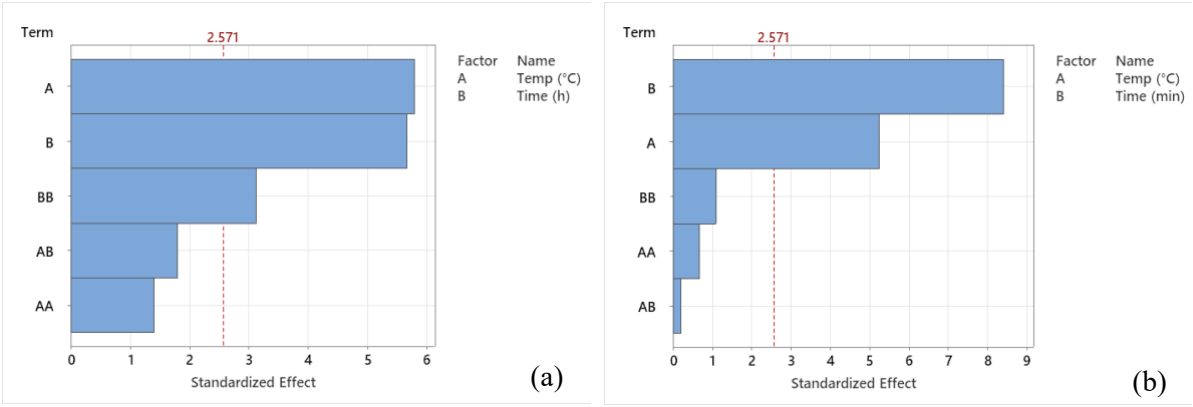

Fig. 5. Pareto charts of the standardized effects of treatment temperature and duration on DMOE of Camphor wood during (a) dry-air heat treatment and (b) hydrothermal heat treatment

For the dry-air heat treatment, treatment temperature and treatment duration were the dominant factors affecting DMOE (Fig. 5a), and both linear terms were highly significant (p = 0.002). In addition, the quadratic effect of treatment duration remained significant (p = 0.026), whereas the interaction between temperature and duration and the quadratic effect of temperature were not statistically significant (p > 0.05). The fitted model explained 94.04% of the experimental variability, with an adjusted R^2 of 88.08% and a predicted R^2 of 58.21%. Although the regression model was statistically significant (p = 0.004), the significant lack-of-fit (p = 0.031) suggests that the quadratic model did not fully capture the response over the investigated experimental region. Therefore, only the statistically significant linear terms were retained in the simplified predictive equation:

$$DMOE\ (GPa) = 14.10 - 0.02394Temp - 0.1171Time \quad (8)$$

where $Temp$ is the treatment temperature (°C), and $Time$ is the treatment duration (h).

For the hydrothermal heat treatment, treatment duration exhibited the greatest standardized effect on DMOE, followed by treatment temperature (Fig. 5b). Both linear terms were highly significant (p < 0.01), whereas the quadratic and interaction terms were not statistically significant (p > 0.05). The fitted model showed good agreement with the experimental data, with an R^2 of 95.22%, an adjusted R^2 of 90.43%, and a predicted R^2 of 70.41%. Moreover, the lack-of-fit was not significant (p = 0.273), indicating that the model adequately represented the experimental responses within the investigated design space. The simplified predictive equation is expressed as:

$$DMOE\ (GPa) = 15.969 - 0.03806Temp - 0.03056Time \quad (9)$$

where $Temp$ is the treatment temperature (°C), and $Time$ is the treatment duration (min).

The response surface and contour plots (Fig. 6a,b) show that DMOE decreased progressively with increasing temperature and treatment duration during dry-air heat treatment. The contour plot further indicates that temperature exerted a slightly greater influence than treatment duration, although both variables contributed substantially to the reduction in DMOE. For the hydrothermal process (Fig. 6c,d), DMOE likewise decreased with increasing treatment temperature and duration, with treatment duration exhibiting the stronger influence, consistent with the Pareto chart. The nearly parallel contour lines further indicate that the interaction between the two processing variables was negligible.

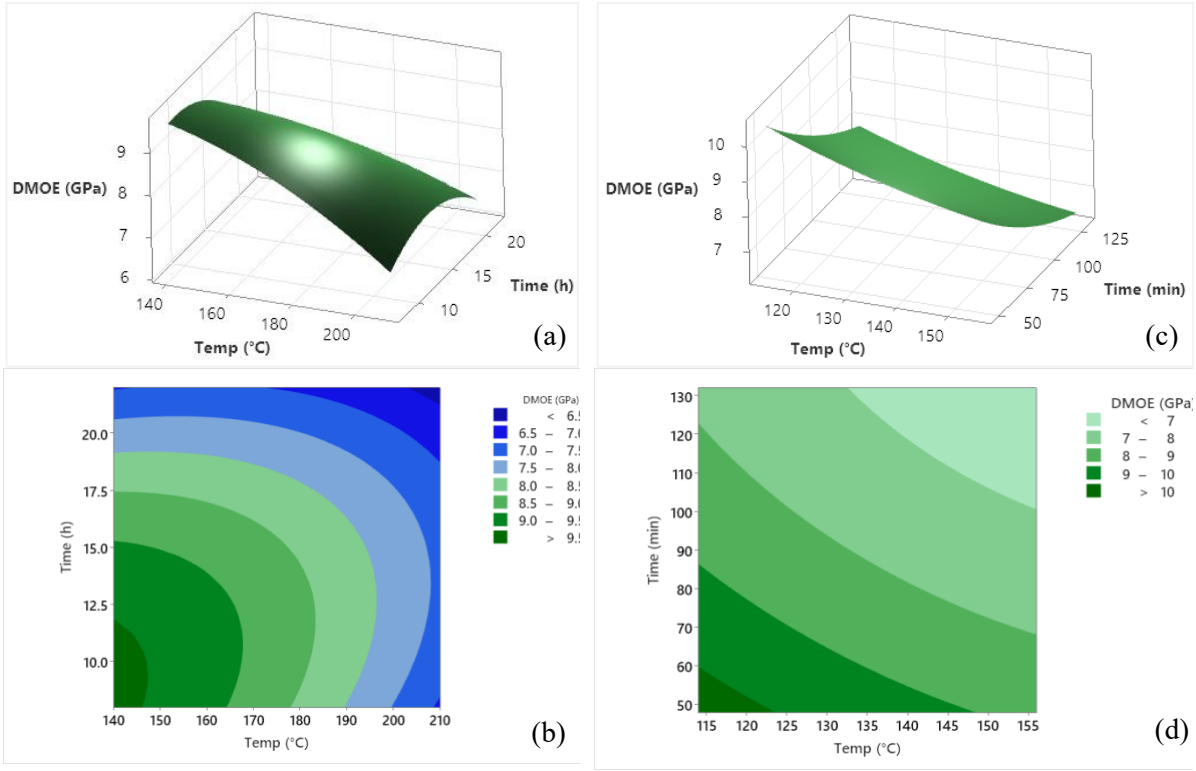

Fig. 6. Response surface and contour plots of DMOE as affected by treatment temperature and duration during (a, b) dry-air heat treatment and (c, d) hydrothermal heat treatment of Camphor wood. Panels (a) and (c) present the response surface plots, whereas panels (b) and (d) present the corresponding contour plots.

The reduction in DMOE after heat treatment can be attributed primarily to the combined effects of changes in air-dry density and the elastic behaviour of the wood cell wall. Since DMOE is calculated as the product of air-dry density and the square of stress wave velocity (Eq. 3), reductions in density resulting from the thermal degradation of hemicelluloses, the degradation or volatilization of extractives, and the release of volatile degradation products contribute directly to lower DMOE values under both dry-air and hydrothermal treatments (Acosta et al., 2021; Esteves & Pereira, 2009; Jančíková & Jablonský, 2025). Thermal modification also induces changes in the wood cell wall, including degradation of hemicelluloses and structural modifications of cellulose and lignin, which can alter its elastic behaviour (Jančíková & Jablonský, 2025). Under hydrothermal conditions, the formation of acetic and formic acids during hemicellulose degradation can further promote polysaccharide degradation and contribute to mass loss (Ali et al., 2021). Consequently, the combined effects of density reduction and heat-induced changes in the cell-wall structure contribute to the overall decrease in DMOE observed with increasing treatment severity. Similar reductions in stress wave-derived dynamic modulus of elasticity have been reported for thermally modified *Eucalyptus grandis*, supporting the use of stress wave-based DMOE as a non-destructive indicator of changes in the dynamic mechanical response of heat-treated wood (Garcia et al., 2012).

Optimal Treatment Conditions

The optimal treatment conditions were determined using a composite desirability function that simultaneously maximized DMOE and AD while minimizing EMC. For the dry-air heat treatment, the optimum condition was predicted at 167 °C for 10 h, with a composite desirability of 0.6370. The corresponding predicted values were 9.0192 GPa for DMOE,

7.27% for EMC, and 0.4925 g/cm³ for AD. For the hydrothermal heat treatment, the optimum condition was predicted at 136 °C for 60 min, with a composite desirability of 0.6529. The predicted DMOE, EMC, and AD were 8.9507 GPa, 9.92%, and 0.5237 g/cm³, respectively (Fig. 7).

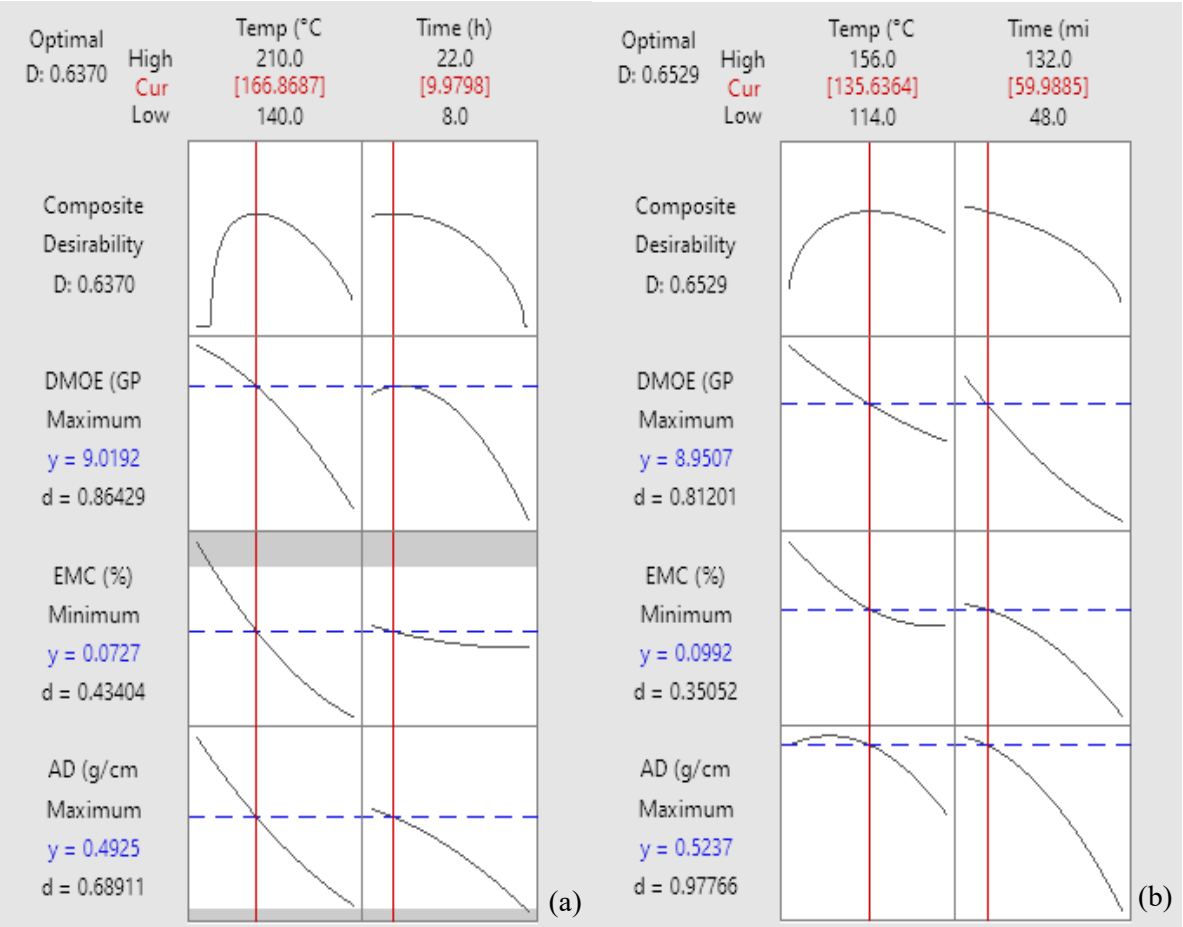

Fig. 7. Optimization plots for the simultaneous maximization of DMOE and AD and minimization of EMC during (a) dry-air heat treatment and (b) hydrothermal heat treatment of Camphor wood

CONCLUSION

Heat treatment reduced the equilibrium moisture content (EMC), air-dry density (AD), and stress wave-based dynamic modulus of elasticity (DMOE) of Camphor wood, with the magnitude of the changes depending on the treatment method, temperature, and duration. The multi-response optimization yielded 167 °C for 10 h for dry-air treatment and 136 °C for 60 min for hydrothermal treatment, with composite desirability values of 0.6370 and 0.6529, respectively. The corresponding predicted values were 7.27% EMC, 0.4925 g/cm³ AD, and 9.0192 GPa DMOE for dry-air treatment, and 9.92% EMC, 0.5237 g/cm³ AD, and 8.9507 GPa DMOE for hydrothermal treatment. The systematic variation in stress wave-derived DMOE with treatment severity indicates that stress wave testing can provide a rapid, non-destructive means of monitoring changes in the dynamic stiffness of heat-treated Camphor wood. These findings provide useful processing conditions for thermal modification of Camphor wood while demonstrating the potential of stress wave-based DMOE as a non-destructive indicator of treatment-induced changes in wood stiffness. Further studies should validate the optimized treatment conditions using independent wood samples and assess the relationship between stress wave-derived DMOE and conventional static mechanical properties.

REFERENCES

Acosta, R., Montoya Arango, J. A., & Da Silva, E. J. (2021). Technologies Applied to Wood Heat Treatments, a Review. *Scientia et Technica*, *26*(2), 129–136. https://doi.org/10.22517/23447214.22641

Ali, Md. R., Abdullah, U. H., Ashaari, Z., Hamid, N. H., & Hua, L. S. (2021). Hydrothermal Modification of Wood: A Review. *Polymers*, *13*(16), 2612. https://doi.org/10.3390/polym13162612

ASTM International. (2025). *Standard Test Methods for Direct Moisture Content Measurement of Wood and Wood-Based Materials* (D4442−20; Version Reapproved 2025). ASTM International. https://doi.org/10.1520/D4442-20R25

Bhuiyan, T. R., & Hirai, N. (2005). Study of crystalline behavior of heat-treated wood cellulose during treatments in water. *Journal of Wood Science*, *51*(1), 42–47. https://doi.org/10.1007/s10086-003-0615-x

Boonstra, M. J., & Tjeerdsma, B. (2006). Chemical analysis of heat treated softwoods. *Holz Als Roh- Und Werkstoff*, *64*(3), 204–211. https://doi.org/10.1007/s00107-005-0078-4

Cipta, H., Kobayashi, K., Chen, S., & Sugiyama, J. (2022). Examination of Cinnamomum camphora interlocked grain adopting X-ray computed tomography combined with particle image velocimetry. *Journal of Wood Science*, *68*(1), 56. https://doi.org/10.1186/s10086-022-02064-z

Del Menezzi, C. H. S., Amorim, M. R. S., Costa, M. A., & Garcez, L. R. O. (2014). Evaluation of Thermally Modified Wood by Means of Stress Wave and Ultrasound Nondestructive Methods. *Materials Science*, *20*(1), 61–66. https://doi.org/10.5755/j01.ms.20.1.3341

Esteves, B. M., & Pereira, H. M. (2009). Wood modification by heat treatment: A review. *BioResources*, *4*(1), 370–404.

Esteves, B., Nunes, L., Lopes, R., & Cruz-Lopes, L. (2025). Enhanced Properties of Cryptomeria japonica (Thunb ex L.f.) D.Don from the Azores Through Heat-Treatment. *Forests*, *16*(1), 166. https://doi.org/10.3390/f16010166

Garcia, R. A., De Carvalho, A. M., De Figueiredo Latorraca, J. V., De Matos, J. L. M., Santos, W. A., & De Medeiros Silva, R. F. (2012). Nondestructive evaluation of heat-treated Eucalyptus grandis Hill ex Maiden wood using stress wave method. *Wood Science and Technology*, *46*(1–3), 41–52. https://doi.org/10.1007/s00226-010-0387-6

Hill, C. A. S. (2006). *Wood Modification: Chemical, Thermal and Other Processes*.

Hill, C., Altgen, M., & Rautkari, L. (2021). Thermal modification of wood—a review: Chemical changes and hygroscopicity. *Journal of Materials Science*, *56*(11), 6581–6614. https://doi.org/10.1007/s10853-020-05722-z

Jančíková, V., & Jablonský, M. (2025). Thermal Modification of Wood—A Review. *Sustainable Chemistry*, *6*(3), 19. https://doi.org/10.3390/suschem6030019

Laskowska, A., Kłosińska, T., & Skirko, D. (2025). Equilibrium moisture content of hydrothermally and thermo-mechanically modified oak wood. *Annals of WULS, Forestry and Wood Technology*, *130*, 16–25. https://doi.org/10.5604/01.3001.0055.4347

Nakagawa, T., Poulin, E., Rueppel, T., Chen, Z., Swinea, J., O'Brien, M., Houser, G., Wood, G., Weinheimer, M., Bahmani, P., Stynoski, P., & Salviato, M. (2024). Effects of thermal modification on the flexure properties, fracture energy, and hardness of western hemlock. *Wood Science and Technology*, *58*(1), 109–133. https://doi.org/10.1007/s00226-023-01511-4

Sun, G. R., He, Y. R., & Wu, Z. H. (2022). Effects of thermal treatment on the dimensional stability and chemical constituents of new and aged camphorwood. *BioResources*, *17*(3), 4186–4195.

Tjeerdsma, B. F., & Militz, H. (2005). Chemical changes in hydrothermal treated wood: FTIR analysis of combined hydrothermal and dry heat-treated wood. *Holz Als Roh- Und Werkstoff*, *63*(2), 102–111. https://doi.org/10.1007/s00107-004-0532-8

Tomak, E. D., & Ermeydan, M. A. (2025). Measuring dimensional stability of thermally modified ayous and iroko wood: Comparison of the three test methods. *Cellulose*, *32*(4), 2581–2597. https://doi.org/10.1007/s10570-025-06404-2

Vidholdová, Z., Dudiak, M., Slabejová, G., & Výbohová, E. (2026). Hydrothermal Modification of Beech Wood. In *Wood Science and Processing Engineering [Working Title]*. IntechOpen. https://doi.org/10.5772/intechopen.1015232

Wang, Y., Wang, Y., Shen, L., Wu, Z., Li, H., Hu, M., Liu, Q., Chen, C., Hu, X., & Zhong, Y. (2023). Evaluation of Wood Anatomical Properties from 18 Tree Species in the Subtropical Region of China. *Forests*, *14*(12), 2344. https://doi.org/10.3390/f14122344

Windadri, F. I., & Rahayu, S. S. B. (1999). Cinnamomum camphora (L.) J.S. Presl. In L. P. A. Oyen & X. D. Nguyen (Eds.), *Plant Resources of South-East Asia No 19: Essential-oil plants*. PROSEA Foundation. https://prosea.prota4u.org/view.aspx?id=655